Journal of Materials Chemistry A

Accepted Manuscript

ROYAL SOCIETY OF CHEMISTRY

www.rsc.org/materialsA

Journal Name

ARTICLE

Hybrid-Dimensional Magnetic Microstructures on 3D Substrates for Remote-Control and Ultrafast Water Remediation

Received 00th January 20xx,
Accepted 00th January 20xx

DOI: 10.1039/x0xx00000x

www.rsc.org/

Ran Du,[a] Qingliang Feng,[a,b] Huaying Ren,[a,c] Qiuchen Zhao,[a] Xin Gao,[a] and Jin Zhang[a,*]

In the field of water remediation, the 3D hydrophobic material with both remote controllability and high oil adsorption performance is highly desirable. To achieve it, magnetic components and microstructures are most likely involved. However, the simple enrolling of magnetic materials always results into quite low adsorption capacity. Additionally, the control of microstructures on 3D materials is immature, which limits the improvement of water/oil selectivity and oil adsorption speed. Herein, we devised the 0D/2D hybrid dimensional magnetic microstructures with well-defined morphology on melamine foams, which providing the magnetism for remote controllability and highly rough surfaces for substantially enhanced water/oil selectivity. Hence, the resultant materials acquired magnetic-driven properties and superhydrophobicity /superoleophilicity simultaneously. Thus, they possess controllable, ultrafast, and high throughput oil uptake ability and high oil/water separation performance. The present strategy may open a new avenue to devise high-performance magnetic 3D assemblies for water remediation.

Introduction

Due to the increasingly aggravated water pollution around the world, the study on water remediation, such as oil/water separation and selective oil uptake is becoming more and more important.[1, 2] In last few years, three-dimensional (3D) hydrophobic/oleophilic materials (3D-HOM) have appeared as rising stars in water remediation, for their promising use in both oil uptake and water/oil separation with high processing capacity.[3-5] A series of 3D substrates based on carbon nanomaterials,[6-12] microporous sponges,[13, 14] commercial foams or sponges, and metal foams[1, 2, 15-18] have been fabricated, which showed high oil adsorption capacity up to 1000 times and excellent oil/water separation performance. Very recently, the elaborate design of microstructures on 3D substrate has also been considered in a few cases,[3, 5, 19] further promoting the performance of water remediation by improving the water/oil selectivity.

On the other hand, to facilitate the handling of 3D-HOM during water purification process and collecting after use, it is desirable to impart remote controllability into materials. For this purpose, one feasible way is to integrate magnetic components in 3D-HOM. In recent years, several works have demonstrated the magnetism integration in 3D networks to produce magnetic-driven sorbents.[20-28] For example, Gui et al.[22] fabricated magnetic carbon nanotubes (CNTs) based sponges by in-situ filling magnetic Fe nanowires into the inner cavity of CNTs during the chemical vapor deposition process, where the magnetic components were permanently integrated and thus ensuring excellent recyclability of resultant materials. However, the magnetism integration and oil adsorption performance in these materials often showed a tradeoff effect. For most works, the magnetic components are simply enrolled for magnetism integration, which is at the expense of density increase of original materials and thus reducing the adsorption capacity.[7] Actually, in average, the maximum oil adsorption capacity of those magnetic 3D-HOM is only about 30 times weight gain, far less than that of conventional 3D-HOM (typically over 100 times weight gain). A few works have been devoted to solve this problem by fabricating low-density materials.[21, 27] For example, Chen et al.[21] prepared ultralight foams (density <5 mg cm^{-3}) by pyrolyzing the metal grafted polyurethane foams, thus oil adsorption capacity over 100 times weight gain. In another work, Kong et al.[27] fabricated iron oxide networks by devising a unique hierarchical macroporous/mesoporous structures, which greatly reduce the density of resultant materials and thus obtaining high adsorption capacity of over 150 times weight gain. However, the more facile synthetic routes, higher oil/water selectivity, and better water remediation performance are still needed to be meet for practical use. Therefore, it is highly desirable and challenging to fabricate 3D-HOM that simultaneously possess remote controllability and high processing capacity in water remediation.

[a] Address here.
[b] Address here.
[c] Address here.
† Footnotes relating to the title and/or authors should appear here.
Electronic Supplementary Information (ESI) available: [details of any supplementary information available should be included here]. See DOI: 10.1039/x0xx00000x

The elaborate engineering of the microstructures on 3D substrates can serve as a feasible way to solve problems above. From the fundamental mechanism, the oil/water selectivity could be significantly improved by introducing suitable microstructures, which is capable of enhancing the surface roughness and thus amplifying the intrinsic wettability of materials towards both water and oil.[29] In this way, the original 3D-HOM could be transformed to superhydrophobic/superoleophilic materials by imparting appropriate microstructures, thus enlarging increasing the water/oil selectivity. Additionally, the increase of the surface roughness can also induce increased Laplace pressure, thereby accelerating the oil adsorption and promoting the adsorption capacity. However, the control of non-magnetic microstructures on 3D materials is still immature, let alone the fine engineering of magnetic microstructures on 3D substrates.

On this basis, we assumed that engineering the magnetic materials into appropriate microstructures on 3D substrate subtly may provide a new way to solve the problem above by simultaneously providing the magnetism for remote control and microstructures for enhancing the oil/water selectivity. Herein, we fabricated a unique 0D/2D hybrid dimensional magnetic microstructure with well-defined morphology, i.e. cobalt-based 2D micrometre-size sheets composed by zero-dimensional (0D) nanometre-size particles on commercial melamine foams (MF), via the combination of controlled precipitation of cobalt (II) ions and reductive annealing. The theoretical calculations showed that this hybrid-dimensional microstructures can dramatically enhance the surface roughness (R_f) up to 6.29, since the apparent R_f is determined by the multiplication of the surface roughness of each dimension, i.e. R_f (R_{f1}, R_{f2})= R_{f1}*R_{f2}. Thus, the water/oil selectivity can be greatly amplified. After a simple vapor deposition process assisted by polydimethylsiloxane (PDMS), the hybrid-dimensional magnetic microstructure based foam with both remote controllability and superhydrophobicity/superoleophilicity (MM-RSF) was obtained. Together with mechanical flexibility inherited from original melamine foam, the resultant material exhibited not only ultrafast selective oil uptake with high capacity (60~160 times of its weight), good recyclability and magnetic-driven properties, but also excellent oil/water separation performance with an efficiency > 99%.

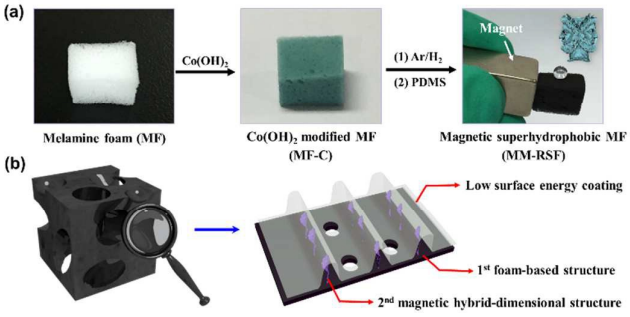

Figure 1. (a) Illustration of synthetic strategy and corresponding digital photos of the material in each step. (b) The demonstration of hierarchical structures of MM-RSF.

Results and discussion

Synthesis and basic characterizations

The synthetic routes is illustrated in **Figure 1a,** including (1) cobalt (II) hydroxide loading by controlled precipitation of cobalt (II) acetate, (2) reductive annealing, and (3) PDMS vapor deposition. By this method, the micrometre-size cobalt (II) hydroxide 2D sheets were introduced first on MF surfaces in step (1) to produce $Co(OH)_2$ loaded foam (MF-C), providing the primary microstructures on MF. Then the 2D cobalt (II) hydroxide sheets were transformed to magnetic cobalt nanoparticles in step (2), accounting for magnetism integration and further enhancement of the surface roughness (the resultant magnetic melamine foam is denoted as MMF). Finally, in step (3), the MMF was coated with low-energy PDMS layer to acquire intrinsically chemical hydrophobicity, thus obtaining superhydrophobic and magnetic melamine foam (MM-RSF). As shown in **Figure 1b**, the MM-RSF showed two-level structures, i.e. several tens micrometre-size porous surface (the first-order structure) provided by original foams and micro/nano hierarchical-size structure (the second-order structure) provided by nanoparticle composed cobalt sheets. In this design, functional microstructures (the second-order structure) are naturally introduced to impart dual functions in materials, i.e. providing high surface roughness for amplification of the intrinsic wettability and integrating magnetism for remote control. In combination with low-energy PDMS coating, the resultant MM-RSF simultaneously acquired superhydrophobicity and magnetism.

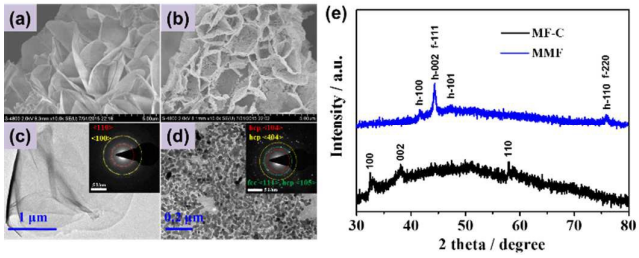

Figure 2. SEM images and TEM images of (a,c) MMF and (b,d) MM-RSF, respectively. Inset in (c,d) are corresponding SAED patterns. (e) The powder XRD patterns of loading matters on MF-C and MMF. In (e), h represents hcp cobalt while f represent fcc cobalt.

As shown in **Figure 2a-d** and **S1,** the morphology evolution during the MM-RSF preparation was revealed by scanning electron microscope (SEM) and transmission electron microscope (TEM). The pristine MF exhibited interconnected macroporous structures with the pore size of several tens micrometres. However, the surface of MF is plain at the magnified scale. After the loading process in step (1), MF surfaces were entirely covered by 2D vertical-aligned cobalt (II)

hydroxide micrometre-size sheets. Both magnified SEM and TEM (**Figure 2c & S1c**) of cobalt (II) hydroxide sheets showed very smooth surfaces. The formation of such smooth sheets can be attributed to the controlled precipitation of cobalt (II) acetate enabled by epichlorohydrin, where the later can serve as the relatively inert proton scavenger and thus releasing the OH^- in a controllable manner.[30, 31] In this way, the $Co(OH)_2$ can slowly develop in a near-equilibrium state, finally forming regular shapes. Additionally, the slowly loading process is also crucial to realize complete diffusion inside the foam and thereby generating uniform microstructures throughout the whole 3D networks. In contrast, rapid precipitation process induced by strong base (potassium hydroxide) not only resulted into uncontrollable rough surfaces (**Figure S2**), but was also unable to achieve uniform loading on 3D substrate.

After reductive annealing, the cobalt (II) hydroxide was converted to ferromagnetic cobalt, which can be verified by selected area electron diffraction (SAED) and powder X-ray diffraction (XRD) (**Figure 2c-e**).[32, 33] By both thermogravimetric (TG) and inductively coupled plasma atomic emission spectrometer (ICP-AES) analysis, the loading amount of cobalt was determined ~20 wt.%. Interestingly, accompanying with chemical reduction process in a "dry" condition, the 2D sheets (several millimetres) converted to the 0D nanoparticles (several tens nanometres) without collapse, resulting into the final 0D/2D micro/nano hierarchical structure much enhanced roughness than that of sole sheet structure. Additionally, the cobalt particles can also impart great magnetism in MF because of their intrinsic high magnetism. Actually, the saturation magnetization of bulk Co (~162 emu g^{-1})[34] is much higher than that of nickel (~58 emu g^{-1})[35] and spinel ferrite Fe_3O_4 (92 emu g^{-1}).[36] As a result, the as-obtained MMF exhibited a quite high saturation magnetization of ~49.2 emu g^{-1}.

Finally, PDMS was coated on the MMF via a facile vapor deposition process[7, 37] for 15 minutes at 235°C, during which a conformal layer following the original morphology of MMF was formed (**Figure S1e,f**). It should be noted that although the as-prepared cobalt on MMF is not stable in air at elevated temperature, the simultaneous deposited PDMS layer can effectively prevent cobalt from deterioration. As evidenced from XRD (**Figure S4**), the cobalt showed considerable oxidation (the appearance of peaks of Co_3O_4 and CoO) after heating alone while minimal oxidation by co-heating with PDMS. In this way, both the magnetism and the micro/nano hierarchical structures of cobalt are preserved after PDMS modification, enabling resultant MM-RSF to simultaneous possess superhydrophobicity and adequate magnetism. Notably, even after metal loading and PDMS coating, the resultant MM-RSF still possess a low density of ~13.9 mg cm^{-3}, comparable to that of nitrogen-doped carbon nanotube aerogels (13.4 mg cm^{-3}),[8] spongy graphene (12±5 mg cm^{-3}),[38] and much lighter than porous polymer aerogels (~30~60 mg cm^{-3}),[13, 14] which was expected to possess good performance in oil uptake.

Superhydrophobicity of MM-RSF

The hydrophobic property of resultant materials was first characterized by static water contact angle measurement (**Figure 3a, S5**). The MM-RSF possessed much higher water contact angle (157.8°) than that of PDMS-coated pristine MF (135.2°) and many other 3D hydrophobic materials without elaborate microstructures engineering. The remarkable superhydrophobicity can be attributed to the high surface roughness provided by elaborately devised 0D/2D hierarchical micro/nano structure. This was further confirmed by the theoretical analysis. As shown in **Figure S6**, for such hierarchical structure, a multiplication rule was adapted to the surface roughness calculation, thus a considerably high roughness of ~6.29 was obtained. Thereby, the hydrophobicity was remarkably amplified by this highly rough surface. At the same time, superoleophilicity was also acquired in MM-RSF, evidenced from an oil contact angle of 0° (**Figure 3b**).

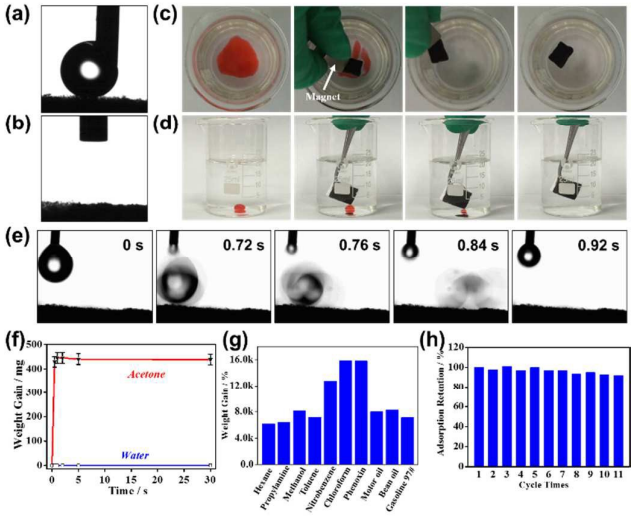

Figure 3. The static contact angle of (a) water and (b) toluene on MM-RSF. (c) On-water and (d) under-water sorption of organic solvents by MM-RSF, respectively. For on-water sorption, a magnet was used to control the motion of MM-RSF. (e) The snapshots of water droplet rolling process on MM-RSF (the substrate was tilted by 3°). (f) The time-dependent sorption behaviour of MM-RSF towards acetone (red) and water (blue). (g) The sorption capacity of MM-RSF towards different organic solvents and oils. (h) The sorption capacity retention of MM-RSF after regeneration by directly heating.

Additionally, the superhydrophobicity of MM-RSF can also be reflected by its low water sliding angle (~9°), fast water rolling process on surface, and significant water repellency during washing (**Figure 3e**, **Movie S1**). Moreover, the water droplet can experience two times bouncing on the surface during the water impacting experiment (**Figure S7-8**), suggesting remarkable water repellency among soft substrates.[39] Apart from superhydrophobicity, MM-RSF also inherit excellent magnetism from MMF (**Figure S9**), facilitating remotely

handling. In fact, MM-RSF can even freely rotate triggered by a normal magnetic stirrer (**Movie S2**). Notably, both the superhydrophobicity and magnetism of the MM-RSF can be well retained after treatment in either high temperature (200°C in air) or low temperature (-196°C in liquid nitrogen) environment (**Figure S10**), enabling their applications in harsh conditions.

Water remediation

Oil adsorption Bearing both remote controllability and remarkable superhydrophobicity/superoleophilicity, MM-RSF can serve as one of the ideal candidates for water remediation. As shown in **Figure 3b-c**, due to ultrahigh water/oil selectivity, MM-RSF can be directly used as adsorbents for rapidly and selectively oil removal either on-water or under-water driving by a magnet. Notably, because of the synergistic effect of fast mass transportation provided by the first-order macroporous structures of MF and much enhanced Laplace pressure provided by second-order micro/nano hierarchical structures, the oil droplets could quickly wet the surface of MM-RSF and then freely transport in the internal 3D networks. In this way, the MM-RSF can not only exhibit an ultrafast oil uptake behaviour (**Movie S3**), but also allow the fully use of the pores inside the foam. As shown in **Figure 3f**, the saturated adsorption can be achieved within 1 s, which is much faster than that of microporous polymer aerogels (over 1 min) and magnetic polyurethane foams (~6 s).[14, 20] The adsorption capacity of MM-RSF towards a series of organic solvents and oils was measured, showing the weight gain of 60~160 times (**Figure 3g**), which is higher than a wide range of polymer sponges or aerogels (13~143 times),[2, 13, 14, 21, 23, 40] although the value is still lower than that of expensive carbon nanotube sponges (80~180 times) and some carbon nanotubes or graphene based aerogels (up to 1000 times).[6, 7, 10, 12] Additionally, the adsorption capacity of MM-RSF stands in front of most reported magnetic sponges.[20-24] The high adsorption capacity can be attributed to the enhanced Laplace pressure induced from the elaborately fabricated microstructures, from which the oil was forced to penetrate into the foam rapidly and thus enabling the full utilization of the pores inside 3D networks. Moreover, thanks to the excellent mechanical flexibility inherited from MF (**Figure S11**), the MM-RSF can be regenerated by either direct heating in air at 100°C or squeezing after oil uptake with a good capacity retention (**Figure 3h & S12**), enabling their recycling use.

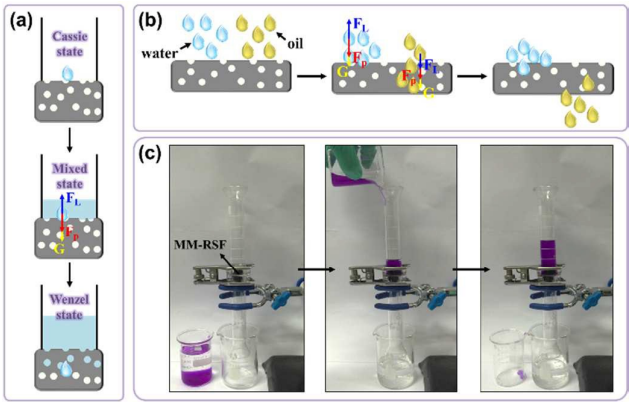

Figure 4. (a) The analysis of Cassie-to-Wenzel state transition with increasing height of water column. (b) The demonstration and force analysis of water and oil droplets during separation process. In (a) and (b), FL refers to Laplace pressure induced by the substrate, Fp refers to experienced static pressure of the target droplet, and G refers to the gravity of the target droplet. (c) The digital photos of oil/water separation process by using MM-RSF as the filter.

Oil/water separation Apart from the selective oil adsorption, the MM-RSF can also serve as the filter for oil/water separation (**Figure 4**). Compared with 2D superhydrophobic substrate or 3D hard substrate (e.g. hydrophobic copper foams[4, 5]), the MM-RSF can not only provide long flowing path to improve the separation efficiency and capacity, but also facilitate easy handling and performance enhancing. The high separation performance of MM-RSF can be explained from the mechanism during oil/water separation process. When the water was dropped on the filter, it was blocked by the Laplace pressure (F_L) generated from the superhydrophobic surface of MM-RSF (**Figure 4a**). If there is only one water droplet on MM-RSF (just like the case for water contact angle measurement), the gravity of droplet (G) can be balanced by the F_L. With increasing water column, the same water droplet will experience increased static pressure (F_p) generated by other water droplets above it (the direction is the same as G), which forced the droplet to wet the substrate and thus causing Wenzel-to-Cassie state transition.[41] After the substrate cannot provide the sufficient F_L to balance $G+F_p$, the water droplet will penetrate the top surface and move to the next surface below it. The filter will finally lose the separation ability when all surfaces are wetted by the water. For 2D filter, the small thickness means fewer available surfaces to resist the water penetration, thus lowing the separation capacity. For 3D filter, there are many replaceable and interconnected superhydrophobic surfaces beneath the top one. Hence, to completely penetrate whole substrate, a very high F_p (i.e. intrusion pressure F_i) is required. This means that the 3D substrate can support a much higher water column than thin 2D substrate, enabling its large processing capacity.

On the other hand, considering the state of oil during separation process (**Figure 4b**), the direction of F_L is in

consistent with G because of superoleophilicity of the substrate, thus causing rapid penetration of oil. After the substrate is completely wetted by the oil, the original PDMS coating will be replaced by the oil layer, which can also repel the water because of the immiscibility of them (this can be evidenced from the high water contact angle of MM-RSF under the oil, see **Figure S13**). In this way, within the intrusion pressure, the oil can be selectively separated from the water. As shown in **Figure 4c**, the oil/water mixture (the hexane was used to represent oil) can be easily separated by using MM-RSF as the filter, and a separation ratio higher than 99% was obtained by using our previously reported method.[5, 14] More importantly, due to the mechanical flexibility of MM-RSF, the separation capacity and efficiency can be easily improved by using stacking several MM-RSF together as the filter.

Conclusions

In summary, by elaborately devising and fabricating hybrid-dimensional magnetic microstructures on the 3D substrate, a remote-controllable and superhydrophobic/superoleophilic melamine foam was facilely prepared. By the combination of controlled precipitation and reductive annealing, a unique 0D/2D hybrid-dimensional cobalt-based microstructure was fabricated on the 3D porous melamine foam, providing both substantially high surface roughness for enhanced oil/water selectivity and magnetic properties for remote controllability. It should be noted that the elaborately devised hybrid-dimensional microstructures can sharply enhance the apparent surface roughness, because the R_f is determined by the multiplication of surface roughness contributed by the each dimension. In next step, the conformal coating of hydrophobic PDMS layer generated the MM-RSF that simultaneously enjoy superhydrophobicity/superoleophilicity and considerable magnetic properties, which showed great potential in both ultrafast, magnetic-driven, and recyclable oil uptake (60~160 times weight gain) and highly efficient oil/water separation (separation ratio > 99%). The presented method may open a new door in intentionally devising high-surface-roughness magnetic 3D substrates and fabricating high-performance, remote controllable 3D-HOM for water remediation.

Experimental

General

All reagents, such as cobalt acetate tetrahydrate and epichlorohydrin were purchased from commercial suppliers (Alfa-Aesar, TCI or Aladdin Chemistry Co.,Ltd.) and used without further purification. The melamine foams were obtained from SINOYQX. Thermogravimetric analysis (TGA) was conducted by Q600 STD with heating rate of 10 K min^{-1} in air or nitrogen. Inductively coupled plasma atomic emission spectrometer (ICP-AES) analysis were conducted using Prodigy7 to determine the cobalt element. Mechanical tests were carried out by a model 3342 Instron Universal Testing Machine equipped with two flat-surface compression plates and a 100 N load cell. The top plate traveling at a speed of 5 mm min^{-1} for normal compressible stress-strain test, 50 mm min^{-1} for loading-unloading cycles. Contact angle measurement was directly conducted on the aerogel at room temperature. The data was collected by OCA20 (Dataphysics). More than five position was measured per sample to receive a mean contact angle. The advancing and receding contact angle were measured by using dispensing and retracting water at a rate of ~ 1.0 µl s^{-1}. The water impact experiment is conducted by dropping a water droplet (~6 µl) from the ~4 cm height, then the snapshots were taken by high-speed camera (~403 fpm). The impact velocity is calculated to be ~88.5 cm s^{-1}.

Preparation of MM-RSF

The melamine foam (MF) was first dropped into the cobalt acetate tetrahydrate aqueous (0.1 M) containing epichlorohydrin (10 vol.%) and heated at 50ºC for ~24 hours. Then the sample was washed with water and frozen at -18ºC in a refrigerator for at least 12 hours before freeze drying for 24 hours, giving rise to cobalt (II) hydroxide loaded melamine foam (MF-C). After then, the dried sample was transferred into a quartz tube and annealed at 350ºC for 1 h under a flow of Ar/H2 of 300/50 (sccm), thus producing cobalt-loaded magnetic melamine foam (MMF). The resultant MMF was further modified by polydimethylsiloxane (PDMS) vapor deposition. In short, MMF was co-heated with PDMS at 235 ºC for 15 minutes in a sealed container, thus creating superhydrophobic and magnetic melamine foam (MM-RSF).

Electron Microscopy

Scanning electron microscopy (SEM) was performed on a Hitachi S-4800 field-emission-gun scanning electron microscope. Transmission electron microscopy (HRTEM) analysis was carried out by Tecnai T20 at 200 kV. The microstructures loaded on the MF were transferred to the ethanol solution by sonication for long hours. Then the samples were prepared by dropping the ethanol dispersion onto carbon coated copper grids and drying at ambient temperature.

Oil Uptake Measurement

Typically, a piece of MM-RSF (ca. 2 mg) was dropped into organic solvent or oil for several hours to achieve completely adsorption equilibrium. Then the weight gain (%) was calculated by

$$q_m=100*(m-m_0)/m_0$$

Where m_0 and m represent the mass of MM-RSF before and after adsorption, respectively. The regeneration of MM-RSF was achieved by either heating at ~100 °C for several minutes or squeezing using a tweezers.

Oil /Water Separation

A piece of MM-RSF (thickness~4 mm) was used as filter and assembled into a separation device as our previously report. In

brief, MM-RSF was sandwiched between two hollow glass-made cylinders with a clamp. The oil/water mixture was prepared by mixing the hexane and deionized water (dyed by xylenol orange) together. For measurement, the oil/water mixture (50 mL, o/w: 4/1) was directly dropped on the separator from the beaker. When the mixed solution went through the separator, the water was selectively blocked while the hexane could easily go through, thus achieving the separation.

Acknowledgements

This work was supported by NSFC (20903009, 50972001, 20725307 and 50821061) and MOST (2011CB932601). Supporting Information is available online from Wiley InterScience or from the author.

Notes and references

[a] Center for Nanochemistry, Beijing National Laboratory for Molecular Sciences, Key Laboratory for the Physics and Chemistry of Nanodevices, State Key Laboratory for Structural Chemistry of Unstable and Stable Species, College of Chemistry and Molecular Engineering, Peking University, Beijing 100871, P.R. China.
E-mail: jinzhang@pku.edu.cn

[b] School of Chemistry and Chemical Engineering, Lanzhou University, Lanzhou 730000, P. R. China

[c] Academy for Advanced Interdisciplinary Studies, Peking University, Beijing 100871, China

Electronic Supplementary Information (ESI) available: Experimental details including thermogravimetric analysis, contact angle measurement, SEM images, etc.. See DOI: 10.1039/c000000x/

1 C. Ruan, K. Ai, X. Li and L. Lu, *Angew. Chem. Int. Ed.*, 2014, **53**, 5556.
2 Y. Gao, Y. S. Zhou, W. Xiong, M. Wang, L. Fan, H. Rabiee-Golgir, L. Jiang, W. Hou, X. Huang and L. Jiang, *ACS Appl. Mater. Interfaces*, 2014, **6**, 5924.
3 R. Du, X. Gao, Q. Feng, Q. Zhao, P. Li, S. Deng, L. Shi and J. Zhang, *Adv. Mater.*, 2015, DOI: 10.1002/adma.201504542.
4 D. Zang, C. Wu, R. Zhu, W. Zhang, X. Yu and Y. Zhang, *Chem. Commun.*, 2013, **49**, 8410.
5 X. Gao, J. Zhou, R. Du, Z. Xie, S. Deng, R. Liu, Z. Liu and J. Zhang, *Adv. Mater.*, 2015, DOI: 10.1002/adma.201504407.
6 X. Gui, J. Wei, K. Wang, A. Cao, H. Zhu, Y. Jia, Q. Shu and D. Wu, *Adv. Mater.*, 2010, **22**, 617.
7 L. Chen, R. Du, J. Zhang and T. Yi, *J. Mater. Chem. A*, 2015, 10.1039/c5ta04370k.
8 R. Du, N. Zhang, J. H. Zhu, Y. Wang, C. Y. Xu, Y. Hu, N. N. Mao, H. Xu, W. J. Duan, L. Zhuang, L. T. Qu, Y. L. Hou and J. Zhang, *Small*, 2015, **11**, 3903.
9 D. D. Nguyen, N.-H. Tai, S.-B. Lee and W.-S. Kuo, *Energy Environ. Sci.*, 2012, **5**, 7908.
10 Y. Zhao, C. Hu, Y. Hu, H. Cheng, G. Shi and L. Qu, *Angew. Chem.*, 2012, **124**, 11533.
11 R. Du, Q. Zhao, N. Zhang and J. Zhang, *Small*, 2015, **11**, 3263.
12 Y. Wu, N. Yi, L. Huang, T. Zhang, S. Fang, H. Chang, N. Li, J. Oh, J. A. Lee, M. Kozlov, A. C. Chipara, H. Terrones, P. Xiao, G. Long, Y. Huang, F. Zhang, L. Zhang, X. Lepró, C. Haines, M. D. Lima, N. P. Lopez, L. P. Rajukumar, A. L. Elias, S. Feng, S. J. Kim, N. T. Narayanan, P. M. Ajayan, M. Terrones, A. Aliev, P. Chu, Z. Zhang, R. H. Baughman and Y. Chen, *Nat Commun*, 2015, **6**, 6141.
13 R. Du, N. Zhang, H. Xu, N. Mao, W. Duan, J. Wang, Q. Zhao, Z. Liu and J. Zhang, *Adv. Mater.*, 2014, **26**, 8053.
14 R. Du, Z. Zheng, N. Mao, N. Zhang, W. Hu and J. Zhang, *Adv. Sci.*, 2015, **2**, 1400006.
15 S. Chen, G. He, H. Hu, S. Jin, Y. Zhou, Y. He, S. He, F. Zhao and H. Hou, *Energy Environ. Sci.*, 2013, **6**, 2435.
16 Y. Yang, Y. Deng, Z. Tong and C. Wang, *J. Mater. Chem. A*, 2014, **2**, 9994.
17 S. Qiu, B. Jiang, X. Zheng, J. Zheng, C. Zhu and M. Wu, *Carbon*, 2015, **84**, 551.
18 Y. Yang, Z. Liu, J. Huang and C. Wang, *J. Mater. Chem. A*, 2015, **3**, 5875.
19 Y. Wang, Y. Shi, L. Pan, M. Yang, L. Peng, S. Zong, Y. Shi and G. Yu, *Nano Lett.*, 2014, **14**, 4803.
20 P. Calcagnile, D. Fragouli, I. S. Bayer, G. C. Anyfantis, L. Martiradonna, P. D. Cozzoli, R. Cingolani and A. Athanassiou, *ACS nano*, 2012, **6**, 5413.
21 N. Chen and Q. Pan, *ACS nano*, 2013, **7**, 6875.
22 X. Gui, Z. Zeng, Z. Lin, Q. Gan, R. Xiang, Y. Zhu, A. Cao and Z. Tang, *ACS Appl. Mater. Interfaces*, 2013, **5**, 5845.
23 L. Wu, J. Zhang, B. Li and A. Wang, *Polym. Chem.*, 2014, **5**, 2382.
24 L. Wu, L. Li, B. Li, J. Zhang and A. Wang, *ACS Appl. Mater. Interfaces*, 2015, **7**, 4936.
25 S. Zhou, W. Jiang, T. Wang and Y. Lu, *Ind. Eng. Chem. Res.*, 2015.
26 A. Turco, C. Malitesta, G. Barillaro, A. Greco, A. Maffezzoli and E. Mazzotta, *J. Mater. Chem. A*, 2015, **3**, 17685.
27 B. Kong, J. Tang, Z. Wu, J. Wei, H. Wu, Y. Wang, G. Zheng and D. Zhao, *Angew. Chem. Int. Ed.*, 2014, **53**, 2888.
28 R. Du, Q. Zhao, P. Li, X. Gao and J. Zhang, 2015, under review.
29 Y. Tian, B. Su and L. Jiang, *Adv. Mater.*, 2014, **26**, 6872.
30 J. W. Long, M. S. Logan, C. P. Rhodes, E. E. Carpenter, R. M. Stroud and D. R. Rolison, *J. Am. Chem. Soc.*, 2004, **126**, 16879.
31 L. Chen, B. Wei, X. Zhang and C. Li, *Small*, 2013, **9**, 2331.
32 Y. Li, L. Li, H. Liao and H. Wang, *J. Mater. Chem.*, 1999, **9**, 2675.
33 H. Ago, Y. Ito, N. Mizuta, K. Yoshida, B. Hu, C. M. Orofeo, M. Tsuji, K.-i. Ikeda and S. Mizuno, *ACS nano*, 2010, **4**, 7407.
34 L. Wu, Q. Li, C. H. Wu, H. Zhu, A. Mendoza-Garcia, B. Shen, J. Guo and S. Sun, *J. Am. Chem. Soc.*, 2015, **137**, 7071.
35 H. Danan, A. Herr and A. Meyer, *J. Appl. Phys.*, 1968, **39**, 669.
36 H.-P. Cong, X.-C. Ren, P. Wang and S.-H. Yu, *ACS nano*, 2012, **6**, 2693.

37 J. Yuan, X. Liu, O. Akbulut, J. Hu, S. L. Suib, J. Kong and F. Stellacci, *Nat. Nanotech.*, 2008, **3**, 332.
38 H. Bi, X. Xie, K. Yin, Y. Zhou, S. Wan, L. He, F. Xu, F. Banhart, L. Sun and R. S. Ruoff, *Adv. Funct. Mater.*, 2012, **22**, 4421.
39 Y. Lu, S. Sathasivam, J. Song, W. Xu, C. J. Carmalt and I. P. Parkin, *J. Mater. Chem. A*, 2014, **2**, 12177.
40 Y. Yang, Z. Liu, J. Huang and C. Wang, *J. Mater. Chem. A*, 2015, **3**, 5875.
41 A. Lafuma and D. Quéré, *Nat. Mater.*, 2003, **2**, 457.

Graphic Abstract

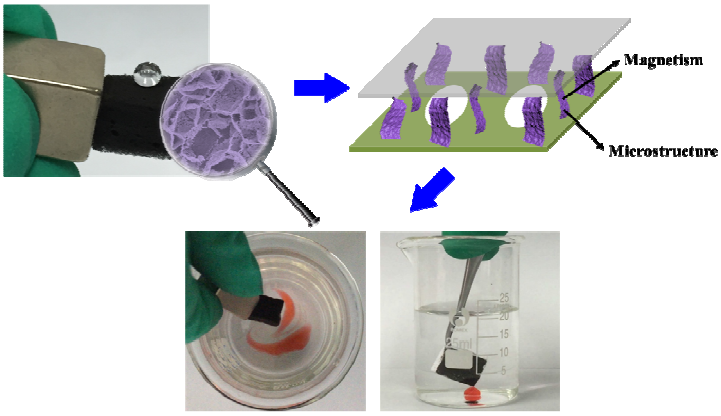

By boosting the surface roughness via devising hybrid-dimensional magnetic microstructures on 3D substrate, the remote controllable and superhydrophobic/superoleophilic melamine foam (MM-RSF) was successfully obtained, showing remarkable magnetic-driven oil sorption behavior and great potential in oil/water separation.